The HapticSpider: a 7-DoF Wearable Device for Cutaneous Interaction with the Palm

Lisheng Kuang[1], Monica Malvezzi[2], Domenico Prattichizzo[2,3], Paolo Robuffo Giordano[1], Francesco Chinello[4], and Claudio Pacchierotti[1]

[1] CNRS, University of Rennes, Inria, IRISA, Rennes, France
[2] University of Siena, Siena, Italy
[3] Italian Institute of Technology, Genova, Italy
[4] Aarhus University, Herning, Denmark

Abstract. This paper introduces a 7-degrees-of-freedom (7-DoF) hand-mounted haptic device, the "HapticSpider". It is composed of a parallel mechanism characterised by eight legs with an articulated diamond-shaped structure, in turn connected to an origami-like shape-changing end-effector. The device can render surface and edge touch simulations as well as apply normal, shear, and twist forces to the palm. This paper presents the device's mechanical structure, a summary of its kinematic model, actuation control, and preliminary device evaluation, characterizing its workspace and force output.

Keywords: Wearable haptics, Cutaneous feedback, Kinematics

1 Introduction

Haptic technology facilitates remote touch in many scenarios, including robotic teleoperation and virtual interaction, but its mainstream use is limited due to non-portable and non-wearable systems, hindering the field's growth [12,13]. In this respect, recent advancements aim to create more wearable and portable haptic solutions, designed for comfort and ease of use [14]. However, while an increasing number of applications leverage haptic capabilities, the stimuli provided by current wearable interfaces remain limited. Balancing realistic touch with cost, wearability, and portability is crucial for advancing haptic technology toward more immersive remote interactions [10,13].

Wearable cutaneous interfaces have been historically designed for the hand, as it is the most sensitive part of our body and the one that is most often used for grasping, manipulation, and probing the environment, especially targeting the fingertip [8,15,5,3,9] or the palm [7,16,2]. The primary benefit of such wearable haptic technology lies in its compact size and lighter weight compared to grounded solutions. These features enable the potential for engaging in various types of haptic interactions in a portable and lightweight manner. However, it is rare to find wearable devices capable of providing multiple haptic sensations, mainly due to limitations in size and weight.

This paper presents a wearable haptic device for the palm, shown in Fig. 1. It features a 7-degrees-of-freedom (7-DoF) end-effector that can move towards/away from the palm, move and rotate on the plane parallel to the user's palm, and

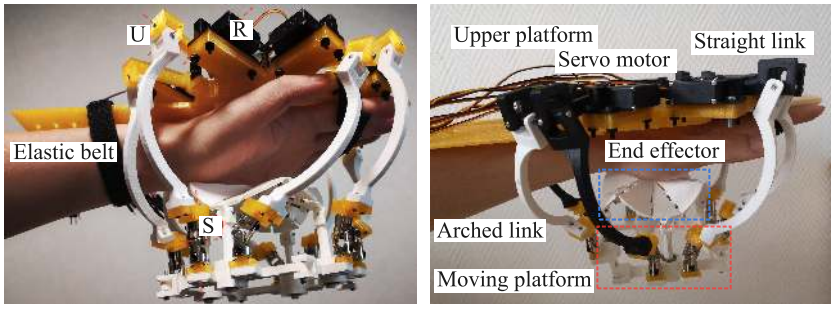

Fig. 1. The proposed 7-DoF haptic device for the palm. Eight actuated legs move the end-effector in all directions/rotations with respect to the palm as well as fold/unfold the origami structure under the user's palm. The fingers are supposed to be straight to bond the strip and to avoid contact with the device legs.

fold along a pre-defined origami-like structure, as shown in Fig. 3. The device is therefore able to elicit the sensation of interacting with a wide range of slanted surfaces and curvatures through combined localized pressure (normal force from the generated flat surfaces and sharp edges), and skin stretch sensations (torsional and shear force).

With respect to other wearable haptic solutions for the palm, such as [7,17,1,2], the proposed device is able to provide a (much) broader range of stimuli, at the cost – however – of a bulkier design.

For example, Malvezzi et al. [8,3] presented a delta-like device for the fingertip that moves a rigid mobile platform thanks to three articulated legs actuated by three servomotors. Williams et al. [18] devised a finger-mounted haptic device with 4-DoF using origami fabrication. This innovative mechanism delivers normal, shear, and torsional haptic feedback to the fingertip. Unlike traditional methods, their approach simplifies joint manufacturing for small devices, reducing complexity and size through origami principles. Addressing the palm, Trinitatova and Tsetserukou [16,17] proposed a 3-DoF inverted delta mechanism consisting of three identical kinematic limbs to move a pin-like end-effector across the palm. Similarly, Dragusanu et al. [4] used a 3-DoF parallel tendon-based mechanical structure to actuate an interchangeable palmar end-effector. Finally, Minamizawa et al. [11] used two motors to actuate two belts moving a flat end-effector on the palm, providing normal and shear forces.

2 Device design and analysis

2.1 The device structure

The device is composed of a static base (upper platform, on the back of the hand) and a moving platform, housing the end-effector in contact with the palm, as shown in Fig. 2a. The upper and moving platforms are connected by eight legs

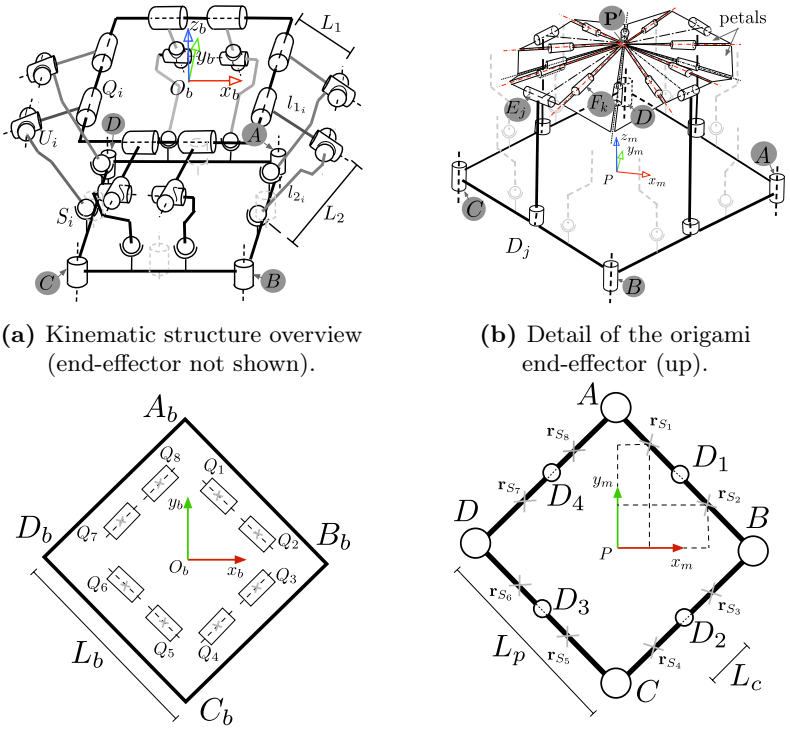

(a) Kinematic structure overview (end-effector not shown).

(b) Detail of the origami end-effector (up).

(c) Planar representation of the static base (upper platform).

(d) Planar representation of the moving platform.

Fig. 2. Device structure. (a, c) The static upper base is square, with edge length L_b and vertices A_b, B_b, C_b, D_b. It houses the revolute joints Q_i connected to links $l_{1,i}$, whose length is L_1. The links are in turn connected via universal joints U_i to links $l_{2,i}$ (length L_2). The spherical joints in S_i connect each leg (composed of $l_{1,i}$ and $l_{2,i}$ links) to the moving platform, which has a diamond shape with vertices A, B, C, D. Such points correspond to revolute joints with parallel axes that make the moving platform articulated. A base reference frame with origin in O_b and axes x_b, y_b, z_b is defined. (b, d) The moving platform houses an origami-like end-effector with vertex P' composed of twelve petals held together with twelve hinge joints F_k ($k = 1, \ldots, 12$). The origami is connected to four additional links with the joints E_j ($j = 1, 2, 3, 4$), which are furthermore connected to the moving platform with joints D_j. An auxiliary reference frame with origin in the center P on the moving platform plane and axes x, y, z is defined to identify the moving platform configuration.

Table 1. Technical specifications of the HapticSpider

Weight	450 g	L × W × H	12 × 12 × 15 cm
Operating voltage	6.0 V	Control system	ESP32
Max normal force	6.0 N	Joint speed	0.14 sec/60°
Max x×y displacement	10×10 cm	Max z displacement	8 cm

(hence, the "spider" reference). These eight identical legs actuate the position, orientation, and configuration of the end-effector mounted on the moving platform.

Each leg is linked to the static upper platform with a revolute joint (Q_i, where $i = \{1, 2, 3, ..., 8\}$) actuated by a servomotor (Hitec HS-85MG). Two rigid links, one straight and shorter ($l_{1,i}$) and one arched and longer ($l_{2,i}$), are serially connected from Q_i to the moving platform through a 2-DoFs universal joint (U_i, between $l_{1,i}$ and $l_{2,i}$) and a final 3-DoF spherical joint S_i, as shown in Fig. 2a. Both the spherical and the universal joints are passive.

The main device features are indicated in Table 1. A video is available as supplemental material, CAD design of the device will be made available on request.

2.2 The origami end-effector

The moving platform is composed of four links with length L_p (see Fig. 2d), interconnected between each other through four passive revolute joints, whose axes pass through A, B, C, D. This structure resembles a diamond-shaped frame whose vertex angles can be varied, i.e. a planar four-bar mechanism.

At the mid-point of each link, a passive revolute joint (D_j with $j = \{1, 2, 3, 4\}$, see Fig. 2b), coaxial with the joints in the vertices, connects the moving platform to an additional link, in turn connected to the origami end-effector through the revolute joint in E_j. The rotation axes of the joints in D_j and E_j are orthogonal. The origami end-effector is the part of the device that contacts the palm, inspired from [6,7]. It is composed of 12 elements, that we call "petals", connected by twelve revolute hinge joints F_k, $k = \{1, 2, 3, ..., 12\}$. Joints F_k are passive, and their rotation angle depends on the distance $\overline{AC}$, and thus $\overline{BD}$, as controlled by the underlying spider structure. In other words, the configuration of the origami structure depends on the deformation of the diamond-shaped frame defined by A, B, C, D joints.

2.3 Inverse kinematics

We indicate with $\mathbf{q} = [q_1, ..., q_8]^{\mathrm{T}}$ the actuators' rotation angles connected to joints Q_i. From Fig. 2d, we indicate with $S_b < O_b, x_b, y_b, z_b >$ the base reference frame and with $S_m < P, x_m, y_m, z_m >$ the local reference frame of the moving platform. The moving platform configuration is defined by the position of point P, $\mathbf{r}_P = [x_P, y_P, z_P]^{\mathrm{T}}$, and the orientation angles, i.e., roll, pitch, yaw angles, collected in the vector $\boldsymbol{\phi} = [\alpha, \beta, \gamma]^{\mathrm{T}}$, both expressed in the base reference

frame S_b. Since the moving platform is not a rigid body, we need a further parameter to represent its opening/closure, due to its diamond-shaped articulated structure. We introduce a further parameter ρ to represent the moving platform shape, defined as half of the diamond diagonal aligned with y_m-axis. The moving platform configuration can be therefore described by the 7-dimensional vector $\mathbf{u} = [x_P, y_P, z_P, \alpha, \beta, \gamma, \rho]^{\mathrm{T}}$. The inverse kinematics defines the relationship mapping $\mathbf{u}$ into $\mathbf{q}$, i.e., $\mathbf{q} = f_d(\mathbf{u})$. According to the above definitions, the coordinates of the diamond vertices A, B, C, D with respect to S_m are

$$\mathbf{r}_A^m = [0, \rho, 0]^T,\ \mathbf{r}_B^m = [\sqrt{L_p^2 - \rho^2},\ 0,\ 0]^T,\ \mathbf{r}_C^m = -\mathbf{r}_A^m,\ \mathbf{r}_D^m = -\mathbf{r}_B^m. \tag{1}$$

For example, when the angles $\angle ABC = \angle BCD = \angle CDA = \angle DAB = \pi/2$ rad (the moving platform is a square), then $\rho = L_p\sqrt{2}/2$. To calculate the coordinates of the spherical joints S_i connecting the moving platform to the legs (see Fig. 2d), we introduce two bi-dimensional auxiliary vectors $\mathbf{a}$ and $\mathbf{b}$:

$$\mathbf{a} = [a_1, a_2] = 1/L_p \left[L_c\sqrt{L_p^2 - \rho^2} + L_0\rho, \quad (L_p - L_c)\sqrt{Lp^2 - \rho^2} + L_0\rho \right]$$
$$\mathbf{b} = [b_1, b_2] = 1/L_p \left[L_c\rho L_0\sqrt{L_p^2 - \rho^2}/L_p \quad (L_p - L_c)\rho L_0\sqrt{L_p^2 - \rho^2} \right].$$

Thanks to $\mathbf{a}$ and $\mathbf{b}$, with simple geometrical considerations, it is possible to express the coordinates of S_i points with respect to S_m, i.e. $\mathbf{r}_{S_i}^m$. Given $\mathbf{R}_{S_m}^{S_b}$ the rotation matrix from the moving platform to the static base, expressed as a function of orientation angles $\boldsymbol{\phi}$ and the position of P, defined by vector $\mathbf{r}_P$, we can easily evaluate the coordinates of the spherical joints with respect to the S_m frame: $\mathbf{r}_{S_i} = \mathbf{r}_P + \mathbf{R}_{S_m}^{S_b}\mathbf{r}_{S_i}^m$.

On the static upper base, the coordinates of the Q_i points, $\mathbf{r}_{Qi}$ can be evaluated in the S_b frame with simple geometrical considerations, as a function of base parameters L_b and L_p indicated in Fig. 2c and Fig. 2d. We introduce eight auxiliary reference frames S_{qi}, with origins in points Q_i, z_i axes parallel to revolute joint axes, and x_i axis on the x_by_b plane. The rotational matrix $\mathbf{R}_{q_i}$ represents the orientation of S_{qi} with respect to S_b. We can then express the coordinates of S_i points for such auxiliary reference frames

$$\mathbf{r}_{S_i} = [s_{p_{x_i}}, s_{p_{y_i}}, s_{p_{z_i}}]^T = \mathbf{R}_{q_i}^T \left[\mathbf{r}_{S_i} - \mathbf{r}_{Qi}\right]^T.$$

This enables us to evaluate the components q_i of the vector joint variables $\mathbf{q}$ as:

$$q_i = 2\arctan\left(\frac{s_{p_{y_i}} + \sqrt{s_{p_{x_i}}^2 + s_{p_{y_i}}^2 - w_i^2}}{w_i + s_{p_{x_i}}}\right)$$

with w_i being an auxiliary variable defined as $w_i = \left(|\mathbf{r}_{S_i}| + L_1^2 - L_2^2\right)/(2L_1)$, where L_{1_i} and L_{2_i} are the same as in Fig. 2a.

As described before, the moving platform is connected to the origami end-effector, which is capable of folding/unfolding, rendering different local shapes on

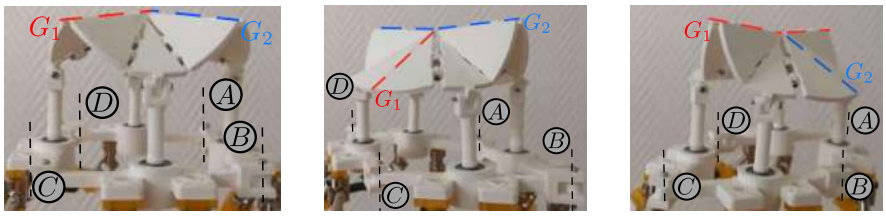

Fig. 3. By changing the configuration of the moving platform, we change the structure of the origami end-effector. For example, in (a), as the distance between the A and C vertices is equal, the origami bends exposing both G_1 and G_2 edges; in (b), as the distance between A and C is maximised while that between B and D is minimised, edge G_2 is more exposed; conversely, in (c), G_1 is more exposed.

the palm. The overall structure is visible in Figs. 2b and 3, and it can be changed by controlling the shape of the underlying moving platform. By controlling position vector $\mathbf{r}_P$ and $\boldsymbol{\phi}$ orientation angles, the position $\mathbf{r}_{P'}$ and orientation of the origami structure can be controlled. By reducing or increasing the distance of the moving platform vertices, through the control of ρ parameter in configuration vector $\mathbf{u}$, it is possible to achieve the two configuration limits shown in Fig. 3b and Fig. 3c. In Fig. 3b, the distance between B and D is maximum, so the edge G_2 is sharp and contacts the palm. On the other hand, in Fig. 3c the distance between A and C is maximized, so this time edge G_1 is sharp and contacts the palm. Fig. 3a shows an intermediate configuration. Specifically, the position of the origami vertex, indicated with P' in Fig. 3b is directly related to P position and moving platform configuration, represented by ρ parameter: $\mathbf{r}^m_{P'} = [0, 0, z^m_{P'}(\rho)]^{\mathrm{T}}$.

2.4 Pilot evaluation

We measured the device performance in providing forces. The device was rigidly fixed to a table and a 6-DoF force-torque sensor (ATI-Nano43) was placed below the static upper base, where the palm should be. The origami end-effector was configured such that $||AC|| = ||BD||$, as in Fig. 3a. Using the inverse kinematics described above, we moved the platform ten times in and out of contact with the ATI sensor, applying a maximum vertical force along the z axis. Results show that the device can apply up to 6 N along this direction.

3 Conclusions

This paper presents a novel wearable haptic device for the palm. It features a 7-DoF end-effector capable of diverse movements. Illustrated in Fig. 1, the device can move towards/away from the palm, traverse and rotate on the plane parallel to the user's palm, and fold along a pre-defined origami-like structure. These capabilities enable the device to simulate interactions with various slanted

surfaces and curvatures by inducing localized pressure and skin stretch sensations. Moreover, as it is very easy to replace end-effector (e.g., using a different foldable origami structure, see also [7]), the device can be quickly adapted to render custom shape sensations.

Compared to existing wearable haptic solutions for the palm, this device offers a significantly wider range of stimuli, rarely seen in a palmar haptic device. However, it does so at the expense of its wearability, suffering from a rather bulky design that severely limits the portability and comfort of the device. We believe that the device could be anyway a useful reference and benchmark system for developing simpler and lighter wearable devices for the hand palm.

Future work will focus on optimising the design by improving the origami structure's mobility, especially for G1 and G2 edges. Mechanical improvements are crucial to optimise the size and shape of the device to reduce the overall encumbrance, reducing the mass, improve the portability and the mechanical stability while providing the desired haptic feedback. We will also try to organise a proper experimental scenario to validate the work, so as to better evaluate the use of the device in relevant cases.

Acknowledgments. We gratefully acknowledge the funding provided by the project "HARIA - Human-Robot Sensorimotor Augmentation - Wearable Sensorimotor Interfaces and Supernumerary Robotic Limbs for Humans with Upper-limb Disabilities" (EU Horizon Europe, GA No. 101070292).

References

1. Altamirano Cabrera, M., Tsetserukou, D.: Linkglide: a wearable haptic display with inverted five-bar linkages for delivering multi-contact and multi-modal tactile stimuli. In: Proc. International AsiaHaptics Conference. pp. 149–154 (2018)
2. Cabrera, M.A., Tirado, J., Heredia, J., Tsetserukou, D.: Linkglide-s: A wearable multi-contact tactile display aimed at rendering object softness at the palm with impedance control in VR and telemanipulation. arXiv preprint arXiv:2208.14149 (2022)
3. Chinello, F., Pacchierotti, C., Malvezzi, M., Prattichizzo, D.: A three revolute-revolute-spherical wearable fingertip cutaneous device for stiffness rendering. IEEE Trans. Haptics **11**(1), 39–50 (2017)
4. Dragusanu, M., Villani, A., Prattichizzo, D., Malvezzi, M.: Design of a wearable haptic device for hand palm cutaneous feedback. Frontiers in Robotics and AI **8**, 706627 (2021)
5. Gabardi, M., Solazzi, M., Leonardis, D., Frisoli, A.: A new wearable fingertip haptic interface for the rendering of virtual shapes and surface features. In: Proc. IEEE Haptics Symposium. pp. 140–146 (2016)
6. Kuang, L., Chinello, F., Giordano, P.R., Marchal, M., Pacchierotti, C.: Haptic mushroom: a 3-dof shape-changing encounter-type haptic device with interchangeable end-effectors. In: Proc. IEEE World Haptics Conference (WHC) (2023)
7. Kuang, L., Ferro, M., Malvezzi, M., Prattichizzo, D., Giordano, P.R., Chinello, F., Pacchierotti, C.: A wearable haptic device for the hand with interchangeable end-effectors. IEEE Trans. Haptics (2023)

8. Malvezzi, M., Chinello, F., Prattichizzo, D., Pacchierotti, C.: Design of personalized wearable haptic interfaces to account for fingertip size and shape. IEEE Trans. Haptics **14**(2), 266–272 (2021)
9. Meli, L., Pacchierotti, C., Salvietti, G., Chinello, F., Maisto, M., De Luca, A., Prattichizzo, D.: Combining wearable finger haptics and augmented reality: User evaluation using an external camera and the microsoft hololens. IEEE Robotics and Automation Letters **3**(4), 4297–4304 (2018)
10. Meli, L., Scheggi, S., Pacchierotti, C., Prattichizzo, D.: Wearable haptics and hand tracking via an rgb-d camera for immersive tactile experiences. In: ACM SIGGRAPH Posters (2014)
11. Minamizawa, K., Kamuro, S., Kawakami, N., Tachi, S.: A palm-worn haptic display for bimanual operations in virtual environments. In: Haptics: Perception, Devices and Scenarios: 6th International Conference, EuroHaptics. pp. 458–463. Springer (2008)
12. Pacchierotti, C., Prattichizzo, D.: Cutaneous/tactile haptic feedback in robotic teleoperation: Motivation, survey, and perspectives. IEEE Trans. Robotics (2024)
13. Pacchierotti, C., Sinclair, S., Solazzi, M., Frisoli, A., Hayward, V., Prattichizzo, D.: Wearable haptic systems for the fingertip and the hand: taxonomy, review, and perspectives. IEEE Trans. Haptics **10**(4), 580–600 (2017)
14. Prattichizzo, D., Otaduy, M., Kajimoto, H., Pacchierotti, C.: Wearable and handheld haptics. IEEE Trans. Haptics **12**(3), 227–231 (2019)
15. Schorr, S.B., Okamura, A.M.: Fingertip tactile devices for virtual object manipulation and exploration. In: Proc. CHI conference on human factors in computing systems. pp. 3115–3119 (2017)
16. Trinitatova, D., Tsetserukou, D.: Deltatouch: a 3d haptic display for delivering multimodal tactile stimuli at the palm. In: Proc. IEEE World Haptics Conference (WHC). pp. 73–78 (2019)
17. Trinitatova, D., Tsetserukou, D.: Touchvr: A wearable haptic interface for vr aimed at delivering multi-modal stimuli at the user's palm. In: SIGGRAPH Asia 2019 XR, pp. 42–43 (2019)
18. Williams, S.R., Suchoski, J.M., Chua, Z., Okamura, A.M.: A 4-dof parallel origami haptic device for normal, shear, and torsion feedback. arXiv preprint arXiv:2109.12134 (2021)